Inorg. Chem. **2002**, *41*, 170–179

Experimental and Theoretical Characterization of Cationic, Neutral, and Anionic Binary Arsenic and Antimony Azide Species

Konstantin Karaghiosoff, Thomas M. Klapötke,* Burkhard Krumm, Heinrich Nöth,† Thomas Schütt, and Max Suter†

Department of Chemistry, Ludwig-Maximilians University of Munich, Butenandtstrasse 5-13 (D), D-81377 Munich, Germany

Received May 1, 2001

Cationic, neutral, and anionic arsenic and antimony halides formed binary arsenic and antimony azide species $M(N_3)_4^+$, $M(N_3)_4^-$, and $M(N_3)_6^-$ (M = As, Sb) upon reaction with trimethylsilyl azide or sodium azide. The compounds were obtained as pure substances or salts, and their identity was established by vibrational spectroscopy and multinuclear NMR spectroscopy and partially by elemental analysis. Attempts to synthesize pentaazides, $M(N_3)_5$ (M = As, Sb), failed due to spontaneous decomposition of the compounds. Density functional theory (B3LYP) was applied to calculate structural and vibrational data. Vibrational assignments of the normal modes for the isolated azide compounds were made on the basis of their vibrational spectra in comparison with computational results. The molecular structures and vibrational spectra of the arsenic and antimony pentaazides have been investigated theoretically. These calculations (B3LYP) show minima structures (NIMAG = 0) for all reported compounds. It is shown that the $M(N_3)_4^+$ (M = As, Sb) cations exhibit ideal S_4 symmetry and the $M(N_3)_6^-$ anions (M = As, Sb) ideal S_6 symmetry. The structure of the hexaazidoarsenate(V) has been determined by X-ray diffraction as its pyridinium salt. [py-H][$As(N_3)_6$] crystallizes in the triclinic space group $P\bar{1}$ with $a = 6.8484(7)$, $b = 7.3957(8)$, and $c = 8.0903(8)$ Å, $\alpha = 91.017(2)$, $\beta = 113.235(2)$, and $\gamma = 91.732(2)°$, $V = 376.29(7)$ Å^3, and $Z = 1$. The structure of the $As(N_3)_6^-$ anion exhibits only S_2 symmetry but shows approximately S_6 symmetry. The calculated and experimentally observed structure as well as the calculated and observed IR and Raman frequencies for all azide species (except $M(N_3)_5$) are in reasonable agreement.

Introduction

The synthesis, isolation, and structural characterization of high-energy compounds is an experimental challenge for chemists.[1] Binary group 15 azides belong to this class of compounds, but only little is known about their synthesis, structures, or properties.[2] However, in a recent study the structures and stabilities of the azidamines $N(N_3)_3$ and $HN(N_3)_2$, the $N(N_3)_2^-$ anion, and the $N(N_3)_4^+$ cation have been theoretically predicted.[3,4] Quite recently, Christe et al. reported the synthesis and properties of the N_5^+ cation.[5] Binary azide species of phosphorus were completely investigated in the 1970s. The binary phosphorus azide species $P(N_3)_3$, $P(N_3)_4^+$, $P(N_3)_5$, and $P(N_3)_6^-$ have been characterized by vibrational methods and ^{31}P NMR spectroscopy, but no structural information is available.[6] The synthesis of the first binary arsenic azide species $As(N_3)_3$ and $As(N_3)_4^+$[7] and the binary antimony azide species $Sb(N_3)_3$[8] and the calculated structures of $As(N_3)_3$ and $Sb(N_3)_3$ were reported.[4] Very

* To whom correspondence should be addressed. Fax: +49-89-2180-7492. E-mail: thomas.m.klapoetke@cup.uni-muenchen.de.

† X-ray structure determination.

(1) (a) Grewer, T. *Thermal Hazards of Chemical Reactions, Industrial Safety Series 4*; Elsevier: Amsterdam, 1994. (b) *Bretherick's Handbook of Reactive Chemical Hazards*, 5th ed.; Butterworth-Heinemann: Oxford, U.K., 1995.

(2) (a) Klapötke, T. M. *Chem. Ber.* **1997**, *130*, 443. (b) Tornieporth-Oetting, I. C.; Klapötke, T. M. *Angew. Chem., Int. Ed. Engl.* **1995**, *34*, 511.

(3) Michels, H. H.; Montgomery, J. A.; Christe, K. O.; Dixon, D. A. *J. Phys. Chem.* **1995**, *99*, 187.

(4) Klapötke, T. M.; Schulz, A. *Main Group Met. Chem.* **1997**, *20*, 325.

(5) Christe, K. O.; Wilson, W. W.; Sheehy, J. A.; Boatz, J. A. *Angew. Chem., Int. Ed. Engl.* **1999**, *38*, 2004.

(6) (a) Buder, W.; Schmidt, A. *Z. Anorg. Allg. Chem.* **1975**, *415*, 263. (b) Schmidt, A. *Chem. Ber.* **1970**, *103*, 3923. (c) Volgnandt, P.; Schmidt, A. *Z. Anorg. Allg. Chem.* **1976**, *425*, 189. (d) Roesky, H. W. *Angew. Chem., Int. Ed. Engl.* **1967**, *6*, 637.

(7) (a) Klapötke, T. M.; Geissler, P. *J. Chem. Soc., Dalton Trans.* **1995**, 3365. (b) Geissler, P.; Klapötke, T. M.; Kroth, H. J. *Spectrochim. Acta* **1995**, *51A*, 1075.

(8) Klapötke, T. M.; Schulz, A.; McNamara, J. *J. Chem. Soc., Dalton Trans.* **1996**, 2985.

10.1021/ic010463l CCC: $22.00
Published on Web 12/22/2001

recently, we have communicated the synthesis, properties, and the first crystal structure of a binary arsenic azide, the $As(N_3)_6^-$ anion, as its tetraphenylphosphonium salt.[9] In this contribution we report on the synthesis, properties, and spectroscopic investigations of further binary cationic and anionic arsenic/antimony azide species and the crystal structure of the pyridinium salt of $As(N_3)_6^-$. Attempted syntheses of $As(N_3)_5$ and $Sb(N_3)_5$ are described. Structures and vibrational data are compared with results of theoretical calculations (B3LYP).

Results and Discussion

Syntheses, Properties, and NMR Spectra of Binary Arsenic and Antimony Azides. The tetraazidostibonium(III) cation, $[Sb(N_3)_4]^+$, was prepared in analogy to the corresponding arsonium salt, $[As(N_3)_4]^+$,[7] by the reaction of $[SbCl_4]^+$ with activated sodium azide in SO_2 solution (eq 1). In addition to this procedure, $[As(N_3)_4]^+$ was prepared by reaction of $[AsCl_4]^+$ with trimethylsilyl azide (see Experimental Section). The concomitant formation of Me_3SiCl or NaCl respectively was observed (also in the following reactions).

$$[SbCl_4][Sb_2F_{11}] + 4NaN_3(\text{act.}) \xrightarrow{SO_2} [Sb(N_3)_4][Sb_2F_{11}] \quad (1)$$

Both cationic azide species are highly explosive solids. At 25 °C both compounds are kinetically stable but explode violently when exposed to a thermal shock test.[10] Crystals of $[As(N_3)_4][AsF_6]$, even when embedded in refrigerated perfluoropolyether oil, pulverized a glass container upon touch. These compounds have to be handled with utmost care. The most useful method for the characterization of covalent azides is ^{14}N NMR spectroscopy. For covalent azide species three well-resolved resonances can be found in the ^{14}N NMR spectra and assignment of the individual resonances to N_α, N_β, and N_γ (connectivity: $M-N_\alpha-N_\beta-N_\gamma$) was made on the basis of arguments given in the literature.[11] The ^{14}N NMR spectra of $[As(N_3)_4][AsF_6]$ and $[Sb(N_3)_4][Sb_2F_{11}]$ in SO_2 show the presence of covalently bonded azides due to the appearance of three signals. $[As(N_3)_4][AsF_6]$ (data in $CDCl_3$; see ref 7) shows signals at δ −137 (N_β), −173 (N_γ), and −279 (N_α), and $[Sb(N_3)_4][Sb_2F_{11}]$ signals at δ −142 (N_β), −173 (N_γ), and −274 (N_α). The spectra show no evidence for azide−fluoride exchange with the anions. The ^{19}F and the ^{75}As NMR spectra of $[As(N_3)_4][AsF_6]$ show only the expected 1:1:1:1 quartet resonance at δ −65.1 (^{19}F) and a binomial septet resonance at δ 0 (^{75}As), indicating the presence of an AsF_6^- anion. No other signals that would indicate a partial or complete azide−fluoride exchange at the anion were detected. The $As(N_3)_4^+$ cation could not be detected in the ^{75}As NMR spectra since, due to the large quadrupole moment of ^{75}As, this nucleus can only be detected in a very symmetrical environment.[12] The first tetrahedrally coordinated arsenic halogen compounds characterized by ^{75}As NMR spectroscopy were the $AsCl_4^+$ and the $AsBr_4^+$ cations recently published by Schrobilgen et al.[13] The ^{19}F NMR spectrum of $[Sb(N_3)_4][Sb_2F_{11}]$ in SO_2 consists of three multiplet resonances at δ −90.5, −98.4, and −128.7, indicating the presence of $Sb_2F_{11}^-$ anions.[14] Similar with $[As(N_3)_4][AsF_6]$, other signals indicative of partial or complete azide−fluoride exchange in the anion could not be detected.

Anionic arsenic(III)/antimony(III) azide species, tetraazidoarsenate(III)/antimonate(III), were synthesized by the reaction of $[Me_4N][AsCl_4]$ and $[Ph_4P][SbCl_4]$ respectively with an excess of Me_3SiN_3 in acetonitrile solution at room temperature:

$$[R][MCl_4] + 4Me_3SiN_3 \xrightarrow{CH_3CN} [R][M(N_3)_4] \quad (2)$$

$$R = Me_4N,\ M = As;\ R = Ph_4P,\ M = Sb$$

Both compounds are kinetically stable and do not explode when exposed to electrical discharge or on contact with a metal spatula. The relative high stabilities of both compounds can probably be explained by the stabilizing effect of large and bulky cations that separate the $M(N_3)_4^-$ anions (M = As, Sb) in the solid state and suppress propagation.[9,15] When samples were exposed to thermal shock, deflagration of tetraazidoarsenate(III)/antimonate(III) occurred. The identity of both compounds was confirmed by elemental analysis. The ^1H and ^{13}C NMR as well as the ^{31}P NMR spectra for $[Ph_4P][Sb(N_3)_4]$ show the expected resonances (see Experimental Section). The ^{14}N NMR spectrum of $[Me_4N][As(N_3)_4]$ shows four resonances, one very sharp signal at δ −135 for N_β, the resonance of N_γ at δ −181, and N_α, as expected, a very broad resonance at δ −326. Further, the sharp resonance at δ −338 can be attributed to the nitrogen atom of the Me_4N^+ cation. For $[Ph_4P][Sb(N_3)_4]$, the ^{14}N NMR spectrum shows signals at δ −136 (N_β), −171 (N_γ), and −324 (N_α).

Reaction of the adduct $As(N_3)_5$·py (py = pyridine) with a solution of HN_3 in CH_2Cl_2 gave yellowish crystals of the hexaazidoarsenate(V) salt [py-H][$As(N_3)_6$]:

$$As(N_3)_5\cdot py + HN_3 \xrightarrow{CH_2Cl_2} [py\text{-}H][As(N_3)_6] \quad (3)$$

The corresponding hexaazidoantimonate(V), $[Sb(N_3)_6]^-$, was

(9) Klapötke, T. M.; Nöth, H.; Schütt, T.; Warchhold, M. *Angew. Chem., Int. Ed. Engl.* **2000**, *39*, 2108.
(10) Tornieporth-Oetting, I. C.; Klapötke, T. M. Covalent Inorganic Non-Metal Azides. In *Combustion Efficiency and Air Quality*; Hargittai, I., Vidoczy, T., Eds.; Plenum Press: New York, 1995; p 51.
(11) (a) Beck, W.; Becker, W.; Chew, K. F.; Derbyshire, W.; Logan, N.; Revitt, D. M.; Sowerby, D. B. *J. Chem. Soc., Dalton Trans.* **1972**, 245. (b) Witanowski, M. *J. Am. Chem. Soc.* **1968**, *90*, 5683. (c) Klapötke, T. M.; Nöth, H.; Schütt, T.; Warchhold, M. *Z. Anorg. Allg. Chem.* **2001**, *627*, 81.
(12) (a) Baliman, G.; Pregosin, P. S. *J. Magn. Reson.* **1977**, *26*, 283. (b) Brevard, C.; Granger, P. *Handbook of High-Resolution Multinuclear NMR*; J. Wiley: New York, Chichester, U.K., 1981; pp 136−137. (c) Mercier, H. P. A.; Sanders, J. C. P.; Schrobilgen, G. J. *J. Am. Chem. Soc.* **1994**, *116*, 2921. (d) Dove, M. F. A.; Sanders, J. C. P.; Jones, E. L.; Parkin, M. J. *J. Chem. Soc., Chem. Commun.* **1984**, 1578.
(13) Gerken, M.; Kolb, P.; Wegner, A.; Mercier, H. P. A.; Borrmann. H.; Dixon, D. A.; Schrobilgen, G. J. *Inorg. Chem.* **2000**, *39*, 2813.
(14) (a) Bacon, J.; Dean, P. A. W.; Gillespie, R. J. *Can. J. Chem.* **1969**, *47*, 1655. (b) LeBlond, N.; Dixon, D. A.; Schrobilgen, G. A. *Inorg. Chem.* **2000**, *39*, 2473.
(15) (a) Neumüller, B.; Schmock, F.; Schlecht, S.; Dehnicke, K. *Z. Anorg. Allg. Chem.* **2000**, *626*, 1792. (b) Beck, W.; Nöth, H. *Chem. Ber.* **1984**, *117*, 419.

prepared analogous to $[As(N_3)_6]^-$ by reaction of $[SbCl_6]^-$ with Me_3SiN_3 in acetonitrile as its tetraethylammonium salt (eq 4). The identity was confirmed by elemental analysis.

$$[Et_4N][SbCl_6] + 6Me_3SiN_3 \xrightarrow{CH_3CN} [Et_4N][Sb(N_3)_6] \quad (4)$$

The explosive properties of these hexaazido anions are similar to those of the tetraazido anions, due to separation of the anions by bulky cations, and $[Ph_4P][As(N_3)_6]$ is kinetically more stable than [py-H]$[As(N_3)_6]$. Although [py-H]$[As(N_3)_6]$ can be handled with relative ease, it explodes violently when exposed to thermal shock, whereas $[Ph_4P]$-$[As(N_3)_6]$ only deflagrates, such as $[Et_4N][Sb(N_3)_6]$. The ^{1}H NMR spectrum of [py-H]$[As(N_3)_6]$ shows in addition to the resonances of the hydrogen atoms of the pyridine ring a broad resonance at δ 13.6, which can be attributed to the hydrogen atom of the protonated nitrogen of pyridinium. The ^{14}N NMR spectrum of [py-H]$[As(N_3)_6]$ indicates covalently bound azides, displaying four signals, three for azide (δ -142 (N_β), -163 (N_γ), and -253 (N_α)) and one broad resonance at δ -167 for pyridinium. The ^{75}As NMR spectrum of [py-H]-$[As(N_3)_6]$ shows a resonance at δ $+12$ ($\Delta_{1/2} = 7000$ Hz) and is near the one of $[Ph_4P][As(N_3)_6]$ (δ $+4$). The ^{1}H and ^{13}C NMR spectra of $[Et_4N][Sb(N_3)_6]$ show the expected resonances (see Experimental Section). The ^{121}Sb NMR spectrum of $[Et_4N][Sb(N_3)_6]$ in DMSO-d_6, where it is only soluble, shows a relatively sharp resonance at δ -3 ($\Delta_{1/2} =$ 500 Hz), indicating the presence of a symmetrical hexacoordinated antimony species in solution. The observed chemical shift appears in the same region as those of SbF_6^- (δ 88) and $SbCl_6^-$ (δ 0).[16] The ^{14}N NMR spectrum shows, in addition to a sharp signal at δ -318 ($\Delta_{1/2} = 2.3$ Hz) of the Et_4N^+ cation, the resonances of covalent azides (δ -141 ($\Delta_{1/2}$ $= 45$ Hz, N_β) and -244 ($\Delta_{1/2} = 580$ Hz, N_α)). But in the characteristic region for the terminal N_γ atom, three signals at δ -154 ($\Delta_{1/2} = 120$ Hz)/-163 ($\Delta_{1/2} = 45$ Hz)/-173 ($\Delta_{1/2}$ $= 110$ Hz) are observed. This might be due to associated antimony azide moieties in solution with bridging N_γ atoms. However, the elemental analysis as well as the vibrational spectra of the solid indicate discrete $Sb(N_3)_6^-$ anions. A similar phenomenon was observed for the palladium azide complex $[Pd(NH_3)_4][Pd(N_3)_4]$.[17]

All attempts to prepare neat $As(N_3)_5$ and $Sb(N_3)_5$ failed and resulted in explosions. These were so intense that only pulverized glass remained. In one experiment AsF_5 was treated with Me_3SiN_3 in SO_2 solution. At ambient temperature the solution can be handled quite safely, but attempts to isolate the material at -78 °C led to violent explosions during the workup procedures. Neat arsenic pentaazide is likely a highly unstable compound, as is arsenic pentachloride.[18] $AsCl_5$ decomposes above -50 °C into $AsCl_3$ and Cl_2, whereas PCl_5 and $SbCl_5$ are stable. The instability of $AsCl_5$ is attributed to d block contraction (post-transition metal effect) and the weakness of the As$-$Cl bond. A synthesis of $Sb(N_3)_5$ has been attempted by two routes. Either SbF_5 or $SbCl_5$ was treated with excess Me_3SiN_3 in SO_2 or CH_2Cl_2 solution. In both cases the reaction mixtures were allowed to warm to ambient temperature, where no visible decomposition or nitrogen evolution occurred. The solvents, resulting $Me_3SiF(Cl)$, and excess Me_3SiN_3 were then removed in vacuo, until no further condensation was visible and a yellowish oil remained. The ^{14}N NMR and Raman spectra in CH_2Cl_2 solution might indicate the formation of a $Me_3SiN_3 \cdot Sb(N_3)_5$ adduct, based on signals attributable to an antimony azide species and trimethylsilyl azide. This adduct seems to be very weak, because evacuating to dryness at room temperature caused explosions, as were observed for $As(N_3)_5$. However, evidence for the formation of a corresponding $Me_3SiN_3 \cdot As(N_3)_5$ adduct could not be detected. This is in good agreement with our studies of nitrogen coordinated Lewis acid$-$base adducts of $As(N_3)_5$ and $Sb(N_3)_5$, where the more stable adducts were formed by $Sb(N_3)_5$.[19]

Vibrational Spectra. Tables 1 and 2 summarize selected computed and experimentally observed frequencies of the here discussed arsenic and antimony azide species. The recorded vibrational data agree well with the theoretical calculations (B3LYP) to allow their assignment. It should be kept in mind that the computations were carried out for single, isolated (gas-phase) molecules. There may well be significant differences between gas phase and solid-state spectra.

For covalent azides, four different vibration modes (ν_{as}-(N_3), $\nu_s(N_3)$, $\delta(N_3)$, and ν(M$-$N)) need to be discussed.[7,9,20] However, frequently 8$-$10 signals can be detected for the azide group in the experimental spectra. A complete assignment of the normal modes is very difficult due to the complex structure of some covalent azides. To give a more detailed assignment of the vibrational modes all binary cationic, neutral and anionic arsenic and antimony azide species were calculated at the B3LYP level of theory.

The vibrational spectra show clearly the presence of azide groups bonded covalently to arsenic or antimony, as demonstrated by the simultaneous appearance of the antisymmetric (ca. 2100 cm^{-1}) and the symmetric (1270 cm^{-1}) azide stretching vibration and the presence of strong As$-$N and Sb$-$N stretching vibrations at 472$-$365 cm^{-1} both in IR and Raman spectra. The antisymmetric stretching vibration of azide should be split if more than one azide group is present in the molecule. This vibration can be divided into the "in-phase" and "out-of-phase" modes. According to calculations the $\nu_{as}(N_3)$ "in-phase" mode appears at higher frequencies than the "out-of-phase" one. As expected, the calculated and observed bands assigned to $\nu_{as}(N_3)$ in the $As(N_3)_4^+$ cation appear at the highest frequencies (see Table 1), followed by the neutral $As(N_3)_5$, with the anionic $As(N_3)_4^-$ and $As(N_3)_6^-$

(16) Mason, J. *Multinuclear NMR*; Plenum Press: New York and London, 1987.
(17) Beck, W.; Klapötke, T. M.; Knizek, J.; Nöth, H.; Schütt, T. *Eur. J. Inorg. Chem.* **1999**, 523.
(18) (a) Seppelt, K. *Z. Anorg. Allg. Chem.* **1977**, *434*, 5. (b) Seppelt, K. *Angew. Chem., Int. Ed. Engl.* **1976**, *15*, 377.
(19) (a) Klapötke, T. M.; Schütt, T. *J. Fluorine Chem.* **2001**, *109*, 151. (b) Klapötke, T. M.; Nöth, H.; Schütt, T.; Warchhold, M. *Z. Anorg. Allg. Chem.* **2001**, *627*, 81.
(20) Revitt, D. M.; Sowerby, D. B. *J. Chem. Soc., Dalton Trans.* **1972**, 847.

Table 1. Selected Observed and Calculated Vibrational Data for Binary Arsenic Azide Species

	$As(N_3)_4^+$ [a]			$As(N_3)_4^-$ [c]			
mode	IR	Ra	calcd[b]	IR	Ra	calcd[b] monomer	calcd[b] dimer
$\nu_{as}(N_3)$ "in-phase"	2129 s	2134 (2)	2312 (288)	2130 s	2121 (4)	2215 (225)	2196 (1132)
$\nu_{as}(N_3)$ "out-of-phase"			2304 (505)		2082 (2)	2193 (2091)	2175 (2370)
$\nu_s(N_3)$ "in-phase"			1248 (455)	1262 m	1258 (1.5)	1350 (103)	1363 (195)
$\nu_s(N_3)$ "out-of- phase"	1245 m	1242 (1)	1247 (276)		1243 (0.5)	1345 (221)	1341 (224)
$\delta(N_3)$ "in-phase"	688 w	698 (1)	681 (57)	676 w		671 (38)	683 (28)
$\delta(N_3)$ "out-of-phase"	662 m		675 (15)	664 m	663 (1)	670 (16)	661 (23)
$\delta(N_3)$ "in-phase/90°"			544 (17)			628 (17)	624 (10)
$\delta(N_3)$ "out-of-phase/90°"			519 (49)	597 w		603 (7)	605 (20)
ν_{as}(AsN)		433 (10)	451 (37)	428 vw	447 (10)	428 (23)	436 (77)
ν_s(AsN)		416 (4)	439 (70)		410 (2)	391 (98)	430 (27)
δ(AsN)		291 (1)	295 (10)		271 (4)	290 (298)	287 (88)

		$As(N_3)_6^-$ [d]		
mode	$As(N_3)_5$: calcd[b]	IR	Ra	calcd[b]
$\nu_{as}(N_3)$ "in-phase"	2267 (643)		2112 (2.5)	2234 (1651)
$\nu_{as}(N_3)$ "out- of-phase"	2259 (936)	2086 s	2081 (1)	2228 (729)
$\nu_s(N_3)$ "in-phase"	1326 (321)	1277 s	1273 (0.5)	1347 (321)
$\nu_s(N_3)$ "out-of- phase"	1283 (404)		1248 (0.5)	1344 (162)
$\delta(N_3)$ "in-phase"	693 (78)			689 (77)
$\delta(N_3)$ "out-of-phase"	684 (44)	666 w	670 (1)	683 (28)
$\delta(N_3)$ "in-phase/90°"	593 (13)			594 (47)
$\delta(N_3)$ "out-of-phase/90°"	581 (15)			592 (7)
ν_{as}(AsN)	452 (108)	418 s	415 (10)	404 (152)
ν_s(AsN)	447 (97)			398 (177)
δ(AsN)	301 (22)		288 (1)	305 (60)

[a] As AsF_6^- salt. [b] In parentheses: IR intensity (km mol^{-1}). [c] As Me_4N^+ salt. [d] As py-H^+ salt.

Table 2. Selected Observed and Calculated Vibrational Data for Binary Antimony Azide Species

	$Sb(N_3)_4^+$ [a]			$Sb(N_3)_4^-$ [c]			
mode	IR	Ra	calcd[b]	IR	Ra	calcd[b] monomer	calcd[b] dimer
$\nu_{as}(N_3)$ "in- phase"		2129 (2)	2279 (318)	2131 w		2248 (712)	2242 (1708)
$\nu_{as}(N_3)$ "out-of- phase"	2113 vs		2274 (640)	2079 m	2084 (2)	2225 (715)	2208 (3280)
$\nu_s(N_3)$ "in-phase"		1286 (1.5)	1249 (405)	1260 s	1273 (0.5)	1358 (155)	1368 (277)
$\nu_s(N_3)$ "out-of- phase"	1260 s		1248 (232)			1350 (147)	1344 (253)
$\delta(N_3)$ "in-phase"	628 s	672 (3.5)	625 (20)	698 m	681 (3)	669 (3)	679 (23)
$\delta(N_3)$ "out-of-phase"			612 (0)	669 w	646 (1)	664 (41)	660 (31)
$\delta(N_3)$ "in-phase/90°"			547 (15)		617 (2)	624 (19)	620 (23)
$\delta(N_3)$ "out-of-phase/90°"			546 (1)			609 (10)	605 (10)
ν_{as}(SbN)			461 (39)		402 (3)	400 (21)	414 (58)
ν_s(SbN)	435 m	421 (10)	454 (35)		365 (2)	372 (80)	342 (72)
δ(SbN)		237 (4.5)	234 (16)		233 (3.5)	232 (35)	232 (306)

		$Sb(N_3)_6^-$ [d]		
mode	$Sb(N_3)_5$: calcd[b]	IR	Ra	calcd[b]
$\nu_{as}(N_3)$ "in-phase"	2262 (362)			2238 (1715)
$\nu_{as}(N_3)$ "out-of-phase"	2256 (1100)	2081 vs	2083 (2.5)	2232 (847)
$\nu_s(N_3)$ "in-phase"	1326 (240)		1298 (1.5)	1351 (324)
$\nu_s(N_3)$ "out-of- phase"	1298 (295)	1256 s		1348 (180)
$\delta(N_3)$ "in-phase"	662 (55)			670 (53)
$\delta(N_3)$ "out-of- phase"	655 (55)	666 w	668 (2.5)	667 (17)
$\delta(N_3)$ "in- phase/90°"	589 (10)			600 (44)
$\delta(N_3)$ "out-of-phase/90°"	585 (12)	576 vw		597 (7)
ν_{as}(SbN)	439 (79)	405 w	412 (10)	404 (106)
ν_s(SbN)	428 (73)		394 (7)	398 (123)
δ(SbN)	250 (30)		226 (3)	233 (73)

[a] As Ph_4P^+ salt. [b] In parentheses: IR intensity (km mol^{-1}). [c] As $Sb_2F_{11}^-$ salt. [d] As Et_4N^+ salt.

being the lowest. The same tendency can be observed in the case of the binary antimony azide species (see Table 2) but is not as distinct as for arsenic azides. This is in good agreement with the calculated N−N distances of all compounds (see the Structures subsection).

The analogous "in-phase"−"out-of-phase" splittings can also be observed for $\nu_s(N_3)$, which appear usually at 1300−1200 cm^{-1}. The reverse trend of what just is mentioned above is detected for this stretching mode: calculated and observed $\nu_s(N_3)$ in the $M(N_3)_4^+$ cations appear at the lowest frequencies, followed by $M(N_3)_5$, with the anionic species $M(N_3)_4^-$ and $M(N_3)_6^-$ (M = As, Sb) exhibiting the highest frequencies. In the case of M = Sb, this trend is again not as pronounced as for M = As.

These results may indicate that Lewis structure **III** (Chart 1) with a higher bond order between N_β and N_γ has higher

Chart 1

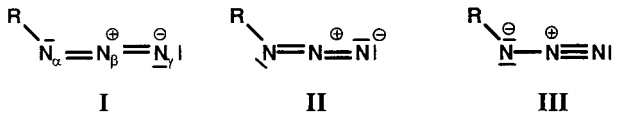

I II III

Chart 2

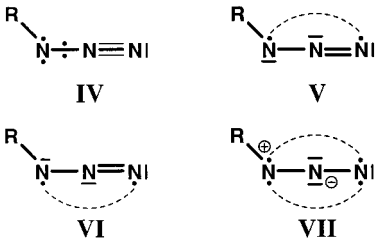

IV V VI VII

weight for azide compounds of the type $M(N_3)_4^+$ and $M(N_3)_5$ than have the Lewis structures **I** and **II** (Chart 1). The situation is reversed for the anionic $M(N_3)_4^-$ and $M(N_3)_6^-$ (M = As, Sb), where structures **I** and **II** with a lower bond order between N_β and N_γ being more important.

In general, it can be shown that when LMOs are used to accommodate the electrons of these bonds in covalent azides, increased valence structure **IV** (Chart 2) is equivalent to resonance between 25 canonical Lewis structures (for R being a mono-atomic univalent group),[21] which include **I**−**III** and **V**−**VII** (Chart 2).[22]

On the basis of calculations, the deformation vibration of the azide group should be split into four signals, due to "in-phase" and "out-of-phase" coupling of the "in-plane" (687−634 cm^{-1}) and "out-of-plane" (617−560 cm^{-1}) deformation. The $\delta(N_3)$ "in-phase" vibration appears at higher frequencies than the $\delta(N_3)$ "out-of-phase" vibration. The arsenic− and antimony−nitrogen stretching vibrations can be divided into a symmetric and an antisymmetric one. The highest frequencies are shown again by the cationic and neutral compounds followed by the anionic species, which is in good agreement with the calculated and observed M−N distances (M = As, Sb). The deformation mode of the As−N bond and Sb−N bond respectively can be assigned to the signals in the region of 291−226 cm^{-1}.

Tables 1 and 2 show exemplary one As−N and one Sb−N deformation vibration. The vibrational spectra all show several As−N and Sb−N deformation vibrations, but definite assignment is not possible, due to combinations of this vibrations with torsion vibrations of the molecules. All reported vibrations agree very well with examples of arsenic and antimony azide species reported in the literature.[7−9,19] Similar tendencies were also observed for $P(N_3)_3$, $P(N_3)_5$, and $P(N_3)_4^+$.[6]

Structures. At the HF level of theory the structures of all binary arsenic and antimony azide compounds were fully optimized in C_1 symmetry resulting in an S_4 symmetry for the $M(N_3)_4^+$ cations, S_6 symmetry for the $M(N_3)_6^-$ anions, C_s symmetry for the monomeric $M(N_3)_4^-$ anions as well as for the neutral $M(N_3)_5$, and S_2 symmetry for the dimeric $M(N_3)_4^-$ anions (M = As, Sb) with no imaginary frequencies (NIMAG = 0). Consequently, the B3LYP computations were performed within S_2, S_4, S_6, and C_s symmetry structure. Selected computed structural parameters for all compounds are compiled in Table 3.

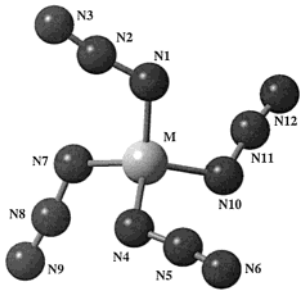

Figure 1. B3LYP-optimized structure of $M(N_3)_4^+$ cations (M = As, Sb).

Figure 2. B3LYP-optimized structure of $M(N_3)_5$ (M = As, Sb).

The $As(N_3)_4^+$ and $Sb(N_3)_4^+$ cations (Figure 1) are surrounded in an almost ideal tetrahedral fashion (ideal S_4 symmetry) by four azide groups. As expected for covalent azides, the azide units display a slightly bent configuration with N−N−N angles of ca. 171.5° for both cationic species. The M−N−N angles are on average 118.7°, e.g. slightly smaller compared to the neutral triazides $M(N_3)_3$, because of different localization of the active lone pair at the N1 atoms compared to the triazides.[4,8] The M−N distances are 1.795 Å for $As(N_3)_4^+$ and 2.009 Å for the $Sb(N_3)_4^+$ cation.

The structures of not isolated $As(N_3)_5$ and $Sb(N_3)_5$ (Figure 2) are characterized by the surrounding of the central atoms with five azide groups in a trigonal bipyramidal fashion. The symmetry of these compounds is lowered from D_{3h} to C_s, however, due to the steric effects of the azide ligands. The N−N−N angles are again slightly bent with an average of 174.6°. In both compounds the N−M−N angles between axial N_α atoms and central atoms are almost linear with 177.2° for $As(N_3)_5$ and 177.4° for $Sb(N_3)_5$. The angles between axial and equatorial N_α atoms are almost 90°, and the angles between the equatorial N_α atoms are in the range of 114.9−123.9° for $As(N_3)_5$ and 112.7−123.7° for $Sb(N_3)_5$, which is typical for a trigonal bipyramidal arrangement. The structures are characterized by two longer M−N distances for the azide ligands in the axial positions (As−N1 1.901, As−N4 1.920 Å; Sb−N1 2.067, Sb−N4 2.080 Å) and three

(21) (a) Harcourt, R. D. *J. Mol. Struct.* **1993**, *300*, 245. (b) Harcourt, R. D.; Sillitoe, J. F. *Aust. J. Chem.* **1974**, *27*, 691.
(22) (a) Harcourt, R. D. *Eur. J. Inorg. Chem.* **2000**, 1901. (b) Klapötke, T. M.; Schulz, A.; Harcourt, R. D. *Quantum Chemical Methods in Main-Group Chemistry*; J. Wiley: New York, 1998.

Table 3. Computed Structural Parameters for the Binary Arsenic and Antimony Azide Species

	$As(N_3)_4^-$	$[As(N_3)_4^-]_2$	$As(N_3)_4^+$	$As(N_3)_5$	$As(N_3)_6^-$
symmetry	C_s	S_2	S_4	C_s	S_6
NIMAG	0	0	0	0	0
zpe/kcal mol^{-1}	32.2	65.5	32.9	41.5	49.7
d(As−N1)/Å	2.058	2.037	1.795	1.901	1.962
d(N1−N2)/Å	1.217	1.216	1.264	1.235	1.224
d(N2−N3)/Å	1.153	1.155	1.127	1.139	1.146
∠(As−N1−N2)/deg	120.9	118.2	118.3	117.2	117.5
∠(N1−N2−N3)/deg	176.7	175.8	171.2	174.6	174.9
∠(N1−As−N4)/deg	172.7	88.5	120.2	177.2	89.5
∠(N1−As−N7)/deg	86.9	87.5	104.4	88.8	90.5
∠(N4−As−N7)/deg	88.5	82.9	104.4	90.5	89.5
	$Sb(N_3)_4^-$	$[Sb(N_3)_4^-]_2$	$Sb(N_3)_4^+$	$Sb(N_3)_5$	$Sb(N_3)_6^-$
symmetry	C_s	S_2	S_4	C_s	S_6
NIMAG	0	0	0	0	0
zpe/kcal mol^{-1}	31.9	63.8	31.5	40.4	48.7
d(Sb−N1)/Å	2.208	2.225	2.009	2.067	2.118
d(N1−N2)/Å	1.218	1.214	1.260	1.236	1.225
d(N2−N3)/Å	1.153	1.157	1.131	1.140	1.146
∠(Sb−N1−N2)/deg	122.7	119.8	119.6	118.3	118.9
∠(N1−N2−N3)/deg	176.4	176.7	172.0	174.3	174.9
∠(N1−Sb−N4)/deg	164.3	90.0	122.3	177.4	88.9
∠(N1−Sb−N7)/deg	84.0	85.1	103.5	89.3	91.1
∠(N4−Sb−N7)/deg	85.7	80.7	103.5	92.3	88.9

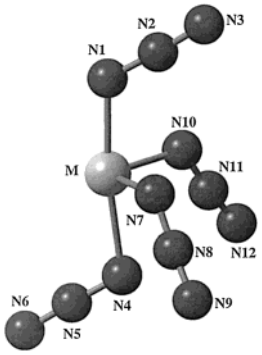

Figure 3. B3LYP-optimized structure of monomeric $M(N_3)_4^-$ anions (M = As, Sb).

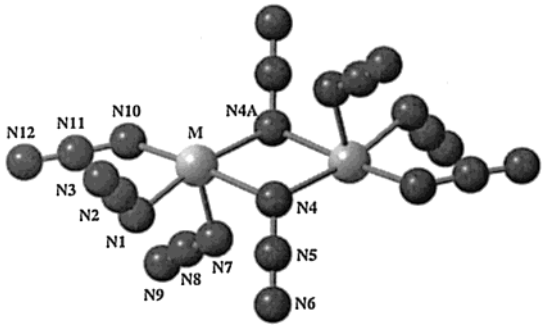

Figure 4. B3LYP-optimized structure of dimeric $M(N_3)_4^-$ anions (M = As, Sb).

shorter M−N distances in the equatorial positions (As−N13 1.860, As−N7/10 1.870 Å; Sb−N13 2.040, Sb−N7/10 2.060 Å).

The tetraazidoarsenate(III)/antimonate(III) have been calculated in a monomeric and a dimeric form, because of the varying nature of crystal structure analyses of tetrahalogeno anions of arsenic and antimony (monomeric or dimeric). While AsX_4^- (X = Cl, Br, I) and $SbCl_4^-$ anions show dimeric structures,[23] the AsF_4^- anion displays a monomeric structure.[24] Monomeric $M(N_3)_4^-$ (M = As, Sb) anions display a Ψ-trigonal bipyramidal structure with ideal C_s symmetry (Figure 3), where the central atoms are surrounded by four azide ligands and one stereochemically active lone pair. Two azides occupy equatorial positions, and two are in axial positions. As predicted by the VSEPR model the lone pair occupies an equatorial position, because it requires more space compared to a bonded pair of electrons. Therefore, the $M(N_3)_4^-$ anions show almost a bisphenoidal (SF_4 type) shape with two longer axial bonds (As−N1 2.058, As−N4 2.205; Sb−N1 2.208, Sb−N4 2.287 Å) and two shorter equatorial bonds (As−N7/10 1.930; Sb−N7/10 2.122 Å). Interesting to note is that one axial azide (N4−N5−N6) has a longer M−N bond compared to the other axial (N1−N2−N3) azide ligand. A possible explanation is a cis orientation of the N4−N5−N6 azide unit toward the lone pair at M, while the other N1−N2−N3 unit is in a trans orientation. The N−M−N angles of the equatorial azide units are within the range of 98.4° (Sb) and 99.1° (As) demonstrating a more repulsive lone pair at M. In both anions the N−M−N angles between the axial N_α atoms and the metal centers are slightly bent with an angle of 172.7° for $As(N_3)_4^-$ and 164.3° for $Sb(N_3)_4^-$ due to this lone pair. The angles between the axial and equatorial N_α atoms are in the range between 84.0 and 88.5° due to the effect of the lone pair in the equatorial position. The calculated structures of the dimeric $[M(N_3)_4^-]_2$ anions exhibit an ideal S_2 symmetry. Two monomeric $M(N_3)_4^-$ units are linked via the N_α atoms of an axial azide (monomeric shape) to form centrosymmetric dimers (Figure 4). The central atoms are surrounded in a Ψ-octahedral fashion by five azide substituents and one lone pair. Four azides occupy equatorial positions, and one azide occupies the axial position. The two axial azides are trans oriented.

(23) (a) Sheldrick, W. S.; Häusler, H.-J.; Kaub, J. *Z. Naturforsch.* **1988**, *43b*, 789. (b) Mohammed, A. T.; Müller, U. *Acta Crystallogr.* **1985**, *C41*, 329. (c) Czado, W.; Rabe, S.; Müller, W. *Z. Naturforsch.* **1998**, *54b*, 288.

(24) Zhang, X.; Seppelt, K. *Z. Anorg. Allg. Chem.* **1997**, *623*, 491.

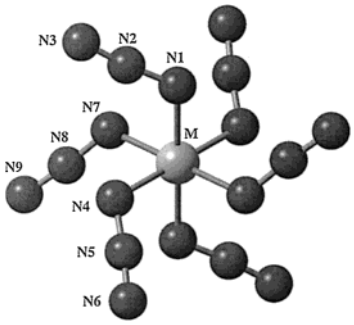

Figure 5. B3LYP-optimized structure of $M(N_3)_6^-$ anions (M = As, Sb).

The M−N distances of the bridging azides are not identical, they are significantly longer (As−N4 2.329, As−N4A 2.499; Sb−N4 2.395, Sb−N4A 2.565 Å) than the distances of the terminal azides (As−N1 2.037, As−N10 2.096; Sb−N1 2.225, Sb−N10 2.279 Å). The M−N10 bond lengths in trans position toward the bridging nitrogen atoms (N4) are again longer than those in cis position (N1). Therefore, the M−N bond lengths show a marked trans effect, which can even be observed in the different M−N10 and M−N1 bond lengths; the latter are shorter and in trans position toward the longer M−N4A bridging bond. The M−N7 bond lengths (As 1.926, Sb 2.098 Å) are not influenced by the trans effect and show therefore shorter M−N7 bond lengths. The N−M−N angles are in the range between 88.8 and 92.3° for both dimeric anions, as one would expect for Ψ-octahedral structures. Interesting to note is that, according to our calculations, the dimerization is energetically not preferred (As 28.5, Sb 34.2 kcal mol^{-1}). However, even the dimeric structures exhibit local minimum structures, and it is important to stress that the calculations were carried out for single anions in the gas phase at 0 K. Dimerization in the solid state can probably be caused by crystal packing or other effects.

For the hexaazido anions of arsenic and antimony local minimum structures were calculated within S_6 symmetry (Figure 5). The calculated structures agree very well with reported crystal structures of hexaazido complexes of arsenic,[9] germanium,[25] tin,[26] lead,[27] and platinum[15a] and the here reported crystal structure of [py-H][As$(N_3)_6$] (vide infra). The central atoms are surrounded by six nitrogen atoms in an octahedral fashion. Azide substituents in trans position are arranged centrosymmetrically. The M−N bond lengths are 1.962 Å for $As(N_3)_6^-$ and 2.118 Å for $Sb(N_3)_6^-$. The azide units are again slightly bent with angles of 174.9° for both anions. The N−M−N angles are in a range between 88.5 and 90.5° for $As(N_3)_6^-$ and 88.9 and 91.1° for $Sb(N_3)_6^-$. The calculated structural parameters for $As(N_3)_6^-$ are in excellent accord with the experimentally observed bond lengths and angles in $[Ph_4P][As(N_3)_6]$[9] and [py-H][As$(N_3)_6$].

Crystal Structure of [py-H][As$(N_3)_6$]. Pyridinium hexaazidoarsenate(V) crystallizes in the triclinic space group $P\bar{1}$ with $Z = 1$. Experimental details of the crystal structure determination are provided in Table 4. The crystal structure reveals the presence of an ionic compound with separated py-H^+ cations and $As(N_3)_6^-$ anions, which do not show any significant cation···anion interactions. Due to the disorder of the cations it was not possible to distinguish between carbon and nitrogen atoms for the pyridine ring. Therefore, all atoms of the pyridine ring were refined as carbon atoms. The molecular structure of the $As(N_3)_6^-$ anion is shown in Figure 6. The anion shows S_2 symmetry (almost S_6 symmetry). The shape, bond lengths, and angles of the experimentally observed molecular structure agree very well with the calculated structure (Figure 5). The arsenic atom occupies an inversion center, and therefore, azide ligands in trans position are oriented in a centrosymmetrical fashion. The As−N bond lengths range from 1.934(4) to 1.940(3) Å, and the N−As−N angles are 86.3(2)−93.7(2)°. While the $N_{\alpha-}N_{\beta}$ bond lengths vary from 1.215(5) to 1.235(5) Å, the terminal $N_{\beta-}N_{\gamma}$ bond lengths are 1.126(5)−1.130(5) Å. The bond angles between the arsenic atom and the azide unit (As−N−N) are in the range of 115.5(3)−116.4(3)°; the angles within the azide unit are slightly bent with angles of 174.7(4)−175.4(4)°. All measured bond lengths and angles are in excellent accord with the values for the $As(N_3)_6^-$ anion

Table 4. Crystal Data and Structure Refinements for [py-H][As$(N_3)_6$]

empirical formula	$C_5H_6AsN_{19}$
fw	405.21
λ(Mo Kα)/Å	0.710 73
cryst system	triclinic
space group	$P\bar{1}$
temp/°C	−80(2)
ρ_{calcd}/g cm^{-3}	1.788
μ/mm^{-1}	2.298
a/Å	6.8484(7)
b/Å	7.3957(8)
c/Å	8.0930(8)
α/deg	91.017(2)
β/deg	113.235(2)
γ/deg	91.732(2)
V/Å^3	376.29(7)
Z	1
R [$I > 4\sigma(I)$][a]	R1 = 0.0402, wR1 = 0.1082
R (all data)	R2 = 0.0405, wR2 = 0.1084

[a] $R = \sum||F_o| - |F_c||/\sum|F_o|$. Refinement method: full-matrix least-squares calculations based on F^2.

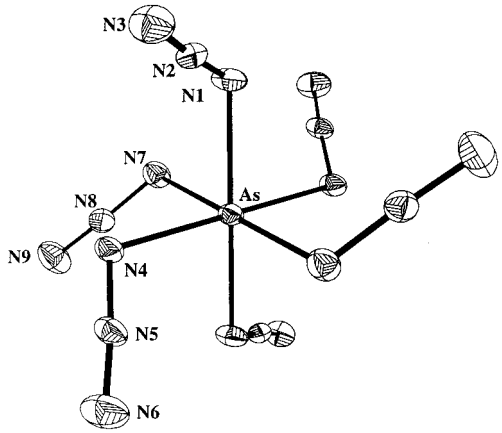

Figure 6. ORTEP plot of the molecular structure of the $As(N_3)_6^-$ anion (pyridinium salt) with thermal ellipsoids at the 25% probability level.

(25) Filippou, A. C.; Portius, P.; Neumann, D. U.; Wehrstedt, K.-D. *Angew. Chem., Int. Ed. Engl.* **2000**, *39*, 4333.
(26) Fenske, D.; Dörner, H.-D.; Dehnicke, K. *Z. Naturforsch.* **1983**, *38b*, 1301.
(27) Polborn, K.; Leidl, E.; Beck, W. *Z. Naturforsch.* **1988**, *43b*, 1206.

in the tetraphenylphosphonium salt.[9] The packing of [py-H][As$(N_3)_6$] is shown in the Supporting Information. The pyridinium cations occupy general positions in the center of the unit cell, and the arsenic atoms are positioned at the midpoint of the *a* axis. Therefore, the anions are arranged in threads, where short N3···N9 (3.286 Å) interactions become visible. This might be a reason for the increased explosive character of this compound compared to [Ph_4P]-[As$(N_3)_6$]. The smaller cation causes increased anion contact and propagation.

Conclusion

Experimental and theoretical studies of the more or less explosive binary arsenic and antimony azide species, $M(N_3)_4^+$, $M(N_3)_4^-$, and $M(N_3)_6^-$ (M = As, Sb), have been performed. A comparison of the calculated structures (density functional theory, B3LYP) reveals significant trends. The cationic species $M(N_3)_4^+$ exhibit the shortest average M−N distances with 1.795 Å for arsenic and 2.009 Å for antimony, followed by neutral $M(N_3)_5$ (As−N 1.884, Sb−N 2.061 Å) compounds. The anionic species show the longest M−N bond lengths, where the anions in the oxidation state V are slightly shorter (As−N 1.962, Sb−N 2.118 Å) compared to the anions in the oxidation state III (monomeric, As−N 2.031, Sb−N 2.185 Å; dimeric As−N 2.177, Sb−N 2.312 Å). In addition to the different M−N bond lengths for cationic, neutral, or anionic species, this tendency is also observed in the same order for the N−N distances within the azide units. The cationic species exhibit the longest $N_\alpha-N_\beta$ and the shortest $N_\beta-N_\gamma$ bond lengths, again followed by the neutral compounds and the anionic species. Consequently, the bond order between N_β and N_γ within the azide unit is highest for $M(N_3)_4^+$, followed by neutral $M(N_3)_5$, whereas $M(N_3)_6^-$ have a greater tendency toward a lower bond order between N_β and N_γ. These results are in good agreement with the experimentally observed and calculated vibrational frequencies as well as with the crystal structure determination of pyridinium hexazidoarsenate(V). The relatively short $N_{\beta-}N_\gamma$ bond lengths for the cationic species which favor nitrogen elimination, might be an explanation for the increased explosive character compared to the anionic compounds.

Experimental Section

CAUTION! *Arsenic and antimony azide compounds are toxic and potentially explosive! They may violently explode under various conditions and should be handled only in small amounts with extreme care. The use of safety equipment like leather gloves, a leather coat, and a face shield is strongly recommended.*

Materials and Apparatus. Activated NaN_3,[28] [$AsCl_4$][AsF_6],[29] [Me_4N][$AsCl_4$],[30] As$(N_3)_5$·py,[19] [$SbCl_4$][Sb_2F_{11}],[31] [Ph_4P][$SbCl_4$],[23] and [Et_4N][$SbCl_6$][32] were prepared by literature methods. A solution of HN_3 in CH_2Cl_2 was prepared by a modified literature method.[33] SbF_5 (Aldrich) was purified by condensation directly into the reaction vessel. AsF_5 (Matheson) and Me_3SiN_3 (Aldrich) were used as received. $SbCl_5$ (Aldrich) was distilled prior to use; SO_2 (Messer-Griesheim) was dried over CaH_2. Solvents were dried by standard methods and freshly distilled prior to use. All compounds reported here are moisture sensitive. Consequently, manipulations were carried out under N_2 using Schlenk techniques or glass vessels fitted with poly(tetrafluoroethylene) valves. Volatile materials were handled in a stainless steel vacuum line, and nonvolatile materials in the dry nitrogen atmosphere of a glovebox.

Computational Methods. The structure and vibrational data for the arsenic and antimony azide species were calculated using the density functional theory with the program package Gaussian 98.[34] The calculations were carried out at the electron-correlated B3LYP level of theory[35] which includes a mixture of Hartree−Fock exchange with DFT exchange-correlation. For N a 6-31G(d) double-ζ basis set was used, and for As and Sb a quasi-relativistic pseudopotential (As, ECP28MWB; Sb, ECP46MWB)[36] and a (5s5p1d)/[3s3p1d]-DZ+P basis set were used.[37] Becke's 3 parameter functional, where the nonlocal correlation is provided by the LYP expression (Lee, Yang, Parr correlation functional), was used, which is implemented in Gaussian 98.

Crystal Structure Determination of [py-H][As$(N_3)_6$]. X-ray single-crystal data of [py-H][As$(N_3)_6$] were collected on a single crystal with the dimensions 0.30 × 0.20 × 0.20 mm on a Siemens P4 diffractometer equipped with a CCD area detector. Data were collected with the hemisphere method and reduced with program SAINT. For absorption correction the program SADABS was used. Structures were solved[38] by heavy atom methods and refined[39] by means of full-matrix least-squares procedures using the SHELX97 programs.

Vibrational Spectra. Infrared spectra were recorded in the range of 4000−300 cm^{-1} on a Perkin-Elmer 983 G IR-spectrometer in substance between KBr plates. Raman spectra were recorded with a Perkin-Elmer Spectrum 2000R NIR FT with the 1064 nm exciting line of a Nd:YAG laser, using sealed glass tubes as sample containers (100−200 mW, 180°, 20 °C).

NMR Spectroscopy. NMR spectra were recorded on a JEOL Eclipse 400 spectrometer at 25 °C at 400.2 MHz (^{1}H), 100.6 MHz (^{13}C), 28.9 MHz (^{14}N), 376.1 MHz (^{19}F), 161.8 MHz (^{31}P), 68.5

(28) Nelles, J. *Ber. Deutsch. Chem. Ges.* **1932**, *65*, 1345.
(29) Minkwitz, R.; Nowicki, J.; Borrmann, H. *Z. Anorg. Allg. Chem.* **1991**, *596*, 93.
(30) Gutmann, V. *Z. Anorg. Allg. Chem.* **1951**, *266*, 331.
(31) Ballard, J. G.; Birchall, T. *Can. J. Chem.* **1978**, *56*, 2947.
(32) Decrassain, R.; Jakubas, R.; Bator, G.; Zaleski, J.; Lefebvre, J.; Kusz, J. *J. Phys. Chem. Solids* **1998**, *59*, 1487.
(33) Fraenk, W.; Habereder, T.; Hammerl, A.; Klapötke, T. M.; Krumm, B.; Mayer, P.; Nöth, H.; Warchhold, M. *Inorg. Chem.* **2001**, *40*, 1334.
(34) Frisch, M. J.; Trucks, G. W.; Schlegel, H. B.; Scuseria, G. E.; Robb, M. A.; Cheeseman, J. R.; Zakrzewski, V. G.; Montgomery, J. A., Jr.; Stratmann, R. E.; Burant, J. C.; Dapprich, S.; Millam, J. M.; Daniels, A. D.; Kudin, K. N.; Strain, M. C.; Farkas, O.; Tomasi, J.; Barone, V.; Cossi, M.; Cammi, R.; Mennucci, B.; Pomelli, C.; Adamo, C.; Clifford, S.; Ochterski, J.; Petersson, G. A.; Ayala, P. Y.; Cui, Q.; Morokuma, K.; Malick, D. K.; Rabuck, A. D.; Raghavachari, K.; Foresman, J. B.; Cioslowski, J.; Ortiz, J. V.; Stefanov, B. B.; Liu, G.; Liashenko, A.; Piskorz, P.; Komaromi, I.; Gomperts, R.; Martin, R. L.; Fox, D. J.; Keith, T.; Al-Laham, M. A.; Peng, C. Y.; Nanayakkara, A.; Gonzalez, C.; Challacombe, M.; Gill, P. M. W.; Johnson, B.; Chen, W.; Wong, M. W.; Andres, J. L.; Gonzalez, C.; Head-Gordon, M.; Replogle, E. S.; Pople, J. A. *Gaussian 98*, revision A.3; Gaussian, Inc.: Pittsburgh, PA, 1998.
(35) (a) Lee, C.; Yang, W.; Parr, R. G. *Phys. Rev.* **1988**, *B37*, 785. (b) Becke, A. D. *Phys. Rev.* **1988**, *A38*, 3098. (c) Miehlich, B.; Savin, A.; Stoll, H.; Preuss, H. *Chem. Phys. Lett.* **1989**, *157*, 200. (d) Becke, A. D. J. *Chem. Phys.* **1993**, *98*, 5648.
(36) Bergner, A.; Dolg, M.; Kuechle, W.; Preuss, H. *Mol. Phys.* **1993**, *80*, 1431.
(37) Kaupp, M.; Schleyer, P. v. R.; Stoll, H.; Preuss, H. *J. Am. Chem. Soc.* **1991**, *113*, 6012.
(38) Sheldrick, G. *SHELXS-97*; University of Göttingen: Göttingen, Germany, 1997.
(39) Sheldrick, G. *SHELXL-97*; University of Göttingen: Göttingen, Germany, 1997.

MHz (^{75}As), and 95.7 MHz (^{121}Sb). The chemical shifts are with respect to $(CH_3)_4Si$ (^{1}H, ^{13}C), CH_3NO_2 (^{14}N), $CFCl_3$ (^{19}F), and 85% H_3PO_4 (^{31}P). The ^{75}As and ^{121}Sb chemical shifts were referenced to $KAsF_6$ (0.1 M in CH_3CN, 25 °C) and $[Et_4N][SbCl_6]$ (0.1 M in CH_3CN, 25 °C) as recommended in ref 16. Typical conditions and parameters for the acquisition of the spectra were the following: ^{14}N NMR, ca. 0.1 M solutions, 10 000 scans, pulse delay 0.2 s, repetition time 0.7 s; ^{75}As and ^{121}Sb NMR, ca. 0.1 M solutions, 10 000 scans, pulse delay 0.2 s, repetition time 0.4 s.

Preparation of $[As(N_3)_4][AsF_6]$. Solutions of $[AsCl_4][AsF_6]$ (0.41 g, 1.0 mmol) in SO_2 (10 mL) and Me_3SiN_3 (0.79 mL, 6.0 mmol) in SO_2 (10 mL) were allowed to react at 25 °C and stirred for 12 h. The solvent and the resulting Me_3SiCl were removed in vacuo, and a yellowish solid remained: yield 0.40 g (92%); IR 2129 (s, $\nu_{as}(N_3)$), 1245 (m, $\nu_s(N_3)$), 702 (vs, $\nu_3(AsF_6)$), 688 (w, $\delta(N_3)$), 662 (m, $\delta(N_3)$), 391 (vs, $\nu_4(AsF_6)$) cm^{-1}; Raman 2134 (2, $\nu_{as}(N_3)$), 1242 (1, $\nu_s(N_3)$), 698 (1, $\delta(N_3)$), 681 (1, $\nu_1(AsF_6)$), 433 (10, ν(AsN)), 416 (4, ν(AsN)), 369 (2, $\nu_5(AsF_6)$), 291 (1, δ(AsN)), 277 (0.5) cm^{-1}; ^{14}N NMR (SO_2) δ −137 (N_β), −173 (N_γ), −279 (N_α); ^{19}F NMR (SO_2) δ −65.1 (q, $^1J_{F-As}$ = 808 Hz); ^{75}As NMR (SO_2) δ 0 (sept, $^1J_{As-F}$ = 849 Hz).

Preparation of $[Me_4N][As(N_3)_4]$. Into a solution of $[Me_4N][AsCl_4]$ (0.09 g, 0.3 mmol) in CH_3CN (40 mL) was added neat Me_3SiN_3 (0.40 mL, 3.0 mmol) at 25 °C. After 10 h of stirring, the solvent and resulting Me_3SiCl were removed in vacuo. $[Me_4N][As(N_3)_4]$, a colorless solid, was obtained in quantitative yield: IR 2922 (s), 2130 (s, $\nu_{as}(N_3)$), 1642 (m), 1483 (s), 1416 (w), 1262 (m, $\nu_s(N_3)$), 1103 (m), 951 (s), 805 (s), 676 (w, $\delta(N_3)$), 664 (m, $\delta(N_3)$), 597 (w, $\delta(N_3)$), 481 (m), 428 (vw, ν(AsN)) cm^{-1}; Raman 3024 (4), 2976 (3), 2121 (4, $\nu_{as}(N_3)$), 2082 (2, $\nu_{as}(N_3)$), 1454 (2.5), 1411 (0.5), 1258 (1.5, $\nu_s(N_3)$), 1243 (0.5, $\nu_s(N_3)$), 951 (1), 757 (2), 663 (1, $\delta(N_3)$), 447 (10, ν(AsN)), 410 (2, ν(AsN)), 271 (4, δ(AsN)), 249 (2.5), 147 (3) cm^{-1}; ^{1}H NMR ($CDCl_3$) δ 3.30 (CH_3); ^{13}C NMR ($CDCl_3$) δ 55.3 (CH_3); ^{14}N NMR ($CDCl_3$) δ −135 (N_β), −181 (N_γ), −326 (N_α), −338 (NMe_4). Anal. Calcd for $C_4H_{12}AsN_{13}$ (317.1): C, 15.2; H, 3.8; N, 57.4. Found: C, 15.5; H, 4.1; N, 56.8.

Preparation of $[py\text{-}H][As(N_3)_6]$. A 1.0 mL volume of a 1 M solution of HN_3 in CH_2Cl_2 was added to a solution of $As(N_3)_5$·py (0.36 g, 1.0 mmol) in CH_2Cl_2 (20 mL) at 25 °C. After 16 h of stirring, the solvent was removed in vacuo. A yellowish solid was obtained. Recrystallization from CH_2Cl_2 at −30 °C gave single crystals suitable for X-ray diffraction: yield 0.31 g (77%); IR 3112 (w), 2086 (s, $\nu_{as}(N_3)$), 1588 (s), 1463 (m), 1277 (s, $\nu_s(N_3)$), 1180 (m), 666 (m, $\delta(N_3)$), 418 (s, ν(AsN)) cm^{-1}; Raman 3112 (0.5), 2112 (2.5, $\nu_{as}(N_3)$), 2081 (1, $\nu_{as}(N_3)$), 1606 (0.5), 1273 (0.5, $\nu_s(N_3)$), 1248 (0.5, $\nu_s(N_3)$), 1198 (0.5), 1011 (1), 670 (1, $\delta(N_3)$), 415 (10, ν(AsN)), 288 (0.5, δ(AsN)), 264 (1.5), 169 (1.5), 113 (2) cm^{-1}; ^{1}H NMR (CD_2Cl_2) δ 13.6 (NH), 8.80/8.57/8.06 (py, 5H); ^{13}C{^{1}H} NMR (CD_2Cl_2) δ 142.6 (C-2), 129.1 (C-4), 126.3 (C-3); ^{14}N NMR (CD_2Cl_2) δ −142 (N_β), −163 (N_γ), −167 (N, py-H), −253 (N_α); ^{75}As NMR (CD_2Cl_2) δ 12.

Attempted Preparation of $As(N_3)_5$. Into a 5 mm NMR tube, closed by a poly(tetrafluoroethylene) valve, was condensed AsF_5 (0.09 g, 0.50 mmol) onto a frozen solution of Me_3SiN_3 (0.40 mL, 3.0 mmol) in 2 mL of SO_2. The reaction mixture was allowed to warm to 25 °C, resulting in a yellow solution. Attempts to separate $As(N_3)_5$, even at −78 °C, from excess of Me_3SiN_3, resulting Me_3SiF, and solvent always ended up in violent explosions.

Preparation of $[Sb(N_3)_4][Sb_2F_{11}]$. Solutions of $[SbCl_4][Sb_2F_{11}]$ (0.72 g, 1.0 mmol) in SO_2 (15 mL) and activated NaN_3 (0.29 g, 4.5 mmol) in SO_2 (10 mL) were allowed to react at 25 °C and stirred for 24 h. The resulting layer on top of a colorless precipitate (unreacted NaN_3, NaCl) was filtered through a fine glass frit, and the SO_2 was removed in vacuo, leaving a colorless solid: yield 0.56 g (76%); IR 2113 (vs, $\nu_{as}(N_3)$), 1628 (m), 1260 (s, $\nu_s(N_3)$), 628 (s, $\delta(N_3)$), 577 (s, $Sb_2F_{11}^-$), 435 (m, ν(SbN)) cm^{-1}; Raman 2129 (2, $\nu_{as}(N_3)$), 1286 (1.5, $\nu_s(N_3)$), 672 (3.5, $\delta(N_3)$), 613 (0.5, $Sb_2F_{11}^-$), 555 (0.5, $Sb_2F_{11}^-$), 421 (10, νSbN), 358 (3), 237 (4.5, δSbN), 140 (3) cm^{-1}; ^{14}N NMR (SO_2) δ −142 (N_β), −173 (N_γ), −274 (N_α); ^{19}F NMR (SO_2) δ −90.5 (m), −98.4 (m), −128.7 (m).

Preparation of $[Ph_4P][Sb(N_3)_4]$. Into a solution of $[Ph_4P][SbCl_4]$ (0.60 g, 1.0 mmol) in CH_3CN (50 mL) was added neat Me_3SiN_3 (0.79 mL, 6.0 mmol) at 25 °C. After 24 h of stirring, the solvent, excess of Me_3SiN_3 and resulting Me_3SiCl were removed in vacuo. $[Ph_4P][Sb(N_3)_4]$ was obtained as a colorless solid: yield 0.52 g (83%); IR 2960 (w), 2919 (m), 2131 (w, $\nu_{as}(N_3)$), 2079 (m, $\nu_{as}(N_3)$), 1448 (m), 1260 (s, $\nu_s(N_3)$), 1091 (m), 1021 (w), 871 (m), 798 (s), 698 (m, $\delta(N_3)$), 669 (w, $\delta(N_3)$), 526 (m) cm^{-1}; Raman 3062 (9), 2963 (3), 2084 (2, $\nu_{as}(N_3)$), 1587 (8), 1273 (0.5, $\nu_s(N_3)$), 1189 (1.5), 1100 (3), 1028 (4.5), 1001 (10), 681 (3, $\delta(N_3)$), 646 (1, $\delta(N_3)$), 617 (2, $\delta(N_3)$), 402 (3, ν(SbN)), 365 (2, ν(SbN)), 333 (2), 233 (3.5, δ(SbN)), 201 (1.5), 101 (6) cm^{-1}; ^{1}H NMR ($CDCl_3$) δ 7.75−7.57 (Ph, m); ^{13}C{^{1}H} NMR ($CDCl_3$) δ 135.7 (C-4), 134.3 (C-3), 130.7 (C-2), 117.7 (C-1); ^{14}N NMR ($CDCl_3$) δ −136 (N_β), −171 (N_γ), −324 (N_α); ^{31}P NMR ($CDCl_3$) δ 23.8 (s). Anal. Calcd for $C_{24}H_{20}PSbN_{12}$ (629.2): C, 45.8; H, 3.2; N, 26.7. Found: C, 45.3; H, 3.5; N, 25.7.

Preparation of $[Et_4N][Sb(N_3)_6]$. Into a solution of $[Et_4N][SbCl_6]$ (0.23 g, 0.5 mmol) in CH_3CN (30 mL) was added neat Me_3SiN_3 (0.79 mL, 6.0 mmol) at 25 °C, resulting in an immediate color change from colorless to yellow. After 24 h of stirring, the solvent, excess Me_3SiN_3, and resulting Me_3SiCl were removed in vacuo. A yellow solid was obtained: yield 0.22 g (86%); IR 3007 (vw), 2993 (w), 2086 (vs, $\nu_{as}(N_3)$), 1484 (s), 1453 (w), 1394 (m), 1256 (s, $\nu_s(N_3)$), 1172 (m), 1000 (s), 784 (s), 666 (w, $\delta(N_3)$), 576 (vw, $\delta(N_3)$), 405 (w, ν(SbN)) cm^{-1}; Raman 2993 (4), 2953 (3), 2083 (2.5, $\nu_{as}(N_3)$), 1460 (3), 1298 (1.5, $\nu_s(N_3)$), 1118 (1.5), 1067 (0.5), 1001 (1), 900 (0.5), 668 (2.5, $\delta(N_3)$), 412 (10, ν(SbN)), 394 (7, ν(SbN)), 301 (3), 226 (3, δ(SbN)), 171 (3.5), 147 (4), 120 (2) cm^{-1}; ^{1}H NMR (DMSO-d_6) δ 3.15 (q, CH_2, $^3J_{H-H}$ = 7.2 Hz), 1.16 (tt, CH_3, $^3J_{N-H}$ = 1.6 Hz); ^{13}C{^{1}H} NMR (DMSO-d_6) δ 51.4 (t, CH_2, $^1J_{C-N}$ = 3.1 Hz), 7.0 (CH_3); ^{14}N NMR (DMSO-d_6) δ −141 (N_β), −163 (t, N_γ), −244 (N_α), −318 (NEt_4); ^{121}Sb NMR (DMSO-d_6) δ −3. Anal. Calcd for $C_8H_{20}SbN_{19}$ (504.1): C, 19.1; H, 4.0; N, 52.8. Found: C, 18.3; H, 3.6; N, 51.2.

Attempted Preparation of $Sb(N_3)_5$. Method a. Into a 5 mm NMR tube, closed by a poly(tetrafluoroethylene) valve, was condensed SbF_5 (0.11 g, 0.50 mmol) onto a frozen solution of Me_3SiN_3 (0.40 mL, 3.0 mmol) in 2 mL of SO_2. The reaction mixture was allowed to warm to 25 °C, resulting in a dark yellow solution. Removal of the solvent, excess of Me_3SiN_3, and resulting Me_3SiF under dynamic vacuum at 25 °C caused explosions.

Method b. Neat Me_3SiN_3 (0.79 mL, 6.0 mmol) was added at −40 °C under stirring to a solution of $SbCl_5$ (0.13 mL, 1.0 mmol) in CH_2Cl_2 (25 mL). After 5 h, the solvent, excess of Me_3SiN_3, and resulting Me_3SiCl were removed in vacuo at 25 °C. Evacuating to dryness caused again violent explosions.

Acknowledgment. Financial support of this work by the University of Munich and the Fonds der Chemischen Industrie is gratefully acknowledged. We are indebted to and thank Prof. Dr. B. Wrackmeyer for his advice regarding the ^{14}N NMR spectra and the Leibnitz Rechenzentrum Munich for a generous allocation of CPU time. We would also like

to thank Dr. M.-J. Crawford who stimulated our interest in the chemistry of As and Sb azides and suggested this study to us.

Supporting Information Available: Tables of crystal data, structure solution and refinement, atomic coordinates, bond lengths and angles, and anisotropic thermal parameters for [py-H][$As(N_3)_6$] in CIF format and figures of the ^{75}As NMR spectrum of [py-H][$As(N_3)_6$] and the ^{14}N NMR spectrum of [Et_4N][$Sb(N_3)_6$] as well as the crystal packing of [py-H][$As(N_3)_6$]. This material is available free of charge via the Internet at http://pubs.acs.org.

IC010463L